

Biosorption of crystal violet and methylene blue dyes using coconut shell powder

Sudhakar S^{1*}, Ahalya N², Saravanan R³ and Sarath Babu M⁴

¹Department of Civil Engineering, Agni College of Technology, Chennai, Tamilnadu, India

²Department of Biotechnology, MS Ramaiah Institute of Technology, Bangalore, Karnataka, India

³Department of Mechanical Engineering, Panimalar Engineering College, Chennai, Tamilnadu, India

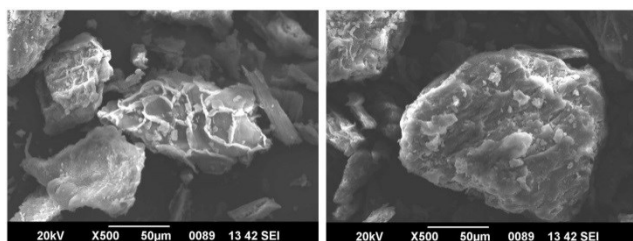
⁴Department of Civil Engineering, PSNA College of Engineering and Technology, Dindigul, Tamilnadu, India

Received: 07/09/2023, Accepted: 21/10/2023, Available online: 07/11/2023

*to whom all correspondence should be addressed: e-mail: sudhakariitm74@gmail.com

<https://doi.org/10.30955/gnj.005364>

Graphical abstract



Abstract

In this study, coconut shell biosorbent was synthesized through chemical processes and activated using concentrated sulfuric acid to serve as an organic adsorbent for the effective removal of dye molecules, particularly Crystal Violet (CV) and Methylene Blue (MB), from wastewater. The biosorbent's surface characteristics, including morphology and functional groups, were comprehensively analyzed using techniques such as BET, FTIR, SEM, and EDX. The experimental investigations revealed that optimal conditions, including a pH of 10.0, biosorbent dosage of 3 g/L, initial dye concentration of 20 mg/L, and a contact time of 60 minutes, led to the efficient removal of 89.74% of CV and 82.32% of MB dye molecules from synthetic solutions. Several isothermal studies were conducted to assess whether the adsorption process exhibited homogeneity or heterogeneity, aiming to gain a deeper understanding of its characteristics. Alongside the aforementioned tests, kinetic investigations were performed to ascertain whether the dye adsorption on the adsorbent was of a physical or chemical nature. Thermodynamic analyses were also undertaken to determine the outward-releasing or inward-absorbing characteristic of the dye adsorption process and to assess its spontaneity. Based on the outcomes of the desorption studies, the addition of 0.3N hydrochloric acid (HCl) resulted in the highest desorption rate. This effectively enhanced the recovery of dye molecules from the exhausted adsorbent, underscoring the effectiveness of

0.3N HCl in facilitating the desorption of adsorbed dye molecules.

Keywords: Biosorption, coconut shells, azo dyes, batch studies, desorption studies.

1. Introduction

Industrial wastewater is a significant source of water pollution, arising from various industries that discharge contaminated water into the environment. This wastewater contains pollutants like heavy metals, toxic chemicals, organic compounds, and other harmful substances, posing serious threats to water quality and aquatic ecosystems. Industries such as manufacturing, chemical processing, mining, textiles, food processing, and oil refineries contribute to this pollution, each releasing specific pollutants based on their operations. The consequences of industrial wastewater pollution are far-reaching. Water bodies near industrial areas become contaminated, making the water unsuitable for human use and supporting aquatic life. Aquatic ecosystems suffer from disrupted biodiversity, and the delicate balance is disturbed, leading to a decline in the number of species (Regti1 *et al.*, 2017). Additionally, exposure to polluted water puts communities at risk of waterborne diseases and long-term health issues, affecting public health. To combat industrial wastewater pollution, effective wastewater treatment processes are essential. Industries need to implement physical, chemical, and biological treatments to remove pollutants before discharging the water. Governments play a critical role in enforcing strict laws and monitoring industrial wastewater discharge to ensure compliance with environmental regulations and prevent water pollution. Encouraging industries to adopt sustainable practices, such as water recycling and reuse, can reduce the volume of wastewater generated and minimize the environmental impact. By taking proactive measures and promoting responsible wastewater management, industries can contribute to a cleaner environment, protect water resources, and safeguard human health and the ecosystems for current and future

generations. Dye removal from water is a critical process in wastewater treatment, environmental protection, and ensuring safe drinking water. Dyes are often used in industries such as textiles, paper, and leather, but they can be harmful to the environment and human health if they are released into water bodies without proper treatment. Dye molecules are typically complex and can resist natural degradation, making their removal a challenging task (Khan *et al.*, 2022). Several methods are employed for dye removal from water: Physical, Chemical, Biological, Advanced Oxidation process, Ion-exchange and Electro chemical methods etc. The choice of dye removal method depends on factors such as the type of dye, its concentration, the volume of water to be treated, and available resources. It's important to note that while these methods can be effective, they might not completely eliminate all traces of dyes. Therefore, a combination of methods or successive treatment steps might be necessary for optimal dye removal and water quality improvement (Syafiuddin *et al.*, 2018).

In this research, Coconut shell powder was utilized as an adsorbent to remove dyes, such as Crystal Violet and Methylene Blue. Coconut shell powder has proven to be an effective adsorbent in removing dyes, including Crystal Violet and Methylene Blue, from waste water. Due to its high surface area and abundant micropores, coconut shell powder offers an ideal environment for adsorption processes. When introduced into dye-contaminated water, the powder acts as a sponge, attracting and trapping dye molecules onto its surface. The porous structure of coconut shell powder provides ample binding sites for the dyes, facilitating their removal from the water. As a result of its natural and eco-friendly properties, coconut shell powder offers a cost-effective and sustainable solution for dye removal in waste water treatment, showing promise as an efficient alternative to conventional adsorbents in combating dye pollution.

2. Materials and methods

2.1. Preparation of adsorbent & stock solution

Coconut shell biochar was prepared as the adsorbent for batch adsorption studies aimed at investigating the removal of crystal violet and methylene blue dyes from aqueous solutions. Clean and dry coconut shells were collected and subjected to carbonization in an oxygen-free environment to convert them into biochar. The resulting biochar was further activated through steam activation to increase its surface area and adsorption capacity. The activated biochar was then ground into a fine powder with uniform particle size through sieving. This preparation process ensured the biochar's purity, porosity, and consistency, making it an effective adsorbent for the dye removal experiments. To prepare the stock solutions of crystal violet and methylene blue, accurate amounts of each dye were weighed using a digital balance. For instance, 0.1 grams of crystal violet and methylene blue were weighed to make 1000 mL of stock solutions, resulting in initial concentrations of 0.1 mg/L. The weighed dyes were dissolved in deionized

water in separate 1000 mL volumetric flasks and thoroughly mixed to ensure complete dissolution. The resulting clear and homogeneous stock solutions were then stored in amber glass bottles to protect them from light and any potential degradation until used in the batch adsorption experiments. These well-prepared stock solutions and coconut shell biochar provided a solid foundation for conducting the adsorption studies and evaluating the efficacy of the biochar as an adsorbent for crystal violet and methylene blue dyes.

2.2. Pore distribution & BET surface area

Nitrogen adsorption-desorption isotherms were utilized to analyze the pore diameter, size dispersion, BET interfacial region, and additional micro and meso voids of Coconut Shell Biochar. These analyses were conducted at -196°C , using nitrogen as the adsorbate for this porous material. The specific surface area of the Coconut Shell Biochar The adsorbent material's specific surface area was ascertained by exposing it to a vacuum at 300°C for a duration of 5 hours in order to eliminate gas molecules, as detailed in the study by Ouyang *et al.* in 2019. The correlation between small-scale and medium-scale voids was established using the Dubinin-Radushkevich (D-R) process, with reference to Equation 1.

$$S_m = S_{BET} - S_u \quad (1)$$

Where,

S_m —mean microscopic void dimension of wastewater residuals

S_u —mean medium-scale void dimension of wastewater residuals

S_{BET} —mean interfacial area determined through BET analysis

With relative pressure of roughly $P/P_0 - 0.99$, the nitrogen requirement for BET analysis and pore volume (V_T) has been obtained. Equation 2 can be used to find out the various sizes of pores available in the coconut shell biosorbent.

$$V_m = V_T - V_u \quad (2)$$

Furthermore, the void width (DP) was computed utilizing equation 3.

$$D_p = \frac{4V_T}{S_{BET}} \quad (3)$$

2.3. Batch adsorption studies

The experimental study was conducted by varying the following parameters: contact time of dyes with Coconut Shell Biochar, the quantity of Coconut Shell Biochar utilized, initial concentration of dyes, pH level, and temperature. Under a consistent temperature of 30°C , the adsorption parameters encompassed factors such as the concentrations of Crystal Violet and Methylene Blue dyes (50mg/100mL), pH levels ranging from 2.0 to 7.0, and Coconut Shell Biochar dosage varying from 0.5 to 2.5 g/L, were studied within the equilibrium period of 60 minutes. The samples containing Coconut Shell Biochar were

subjected to a 60-minute agitation in a rotary shaker to achieve equilibrium. After 20 minutes of ideal condition, the interaction period between the dyes and the adsorbent was changed meticulously throughout a time span ranging from 10 minutes to 2 hours. Subsequently, the quantity of dyes adsorbed by the Coconut Shell Biochar adsorbent was evaluated at various time intervals using Equation 4.

$$q_t = \frac{(C_o - C_t) V}{m} \text{ mg/g} \quad (4)$$

q_t – Cumulative quantity of dyes adsorbed by Coconut Shell Biochar (mg/g).

C_t – Sequential adsorption procedure and its content level

V – Magnitude of the liquid mixture

M – Weight of the adsorption substance

The conical flask remains were collected and subjected to Atomic Absorption Spectroscopy (AAS) examination to determine the proportion of dyes (Crystal Violet and Methylene Blue) absorbed by Coconut Shell Biochar. To ensure accuracy, each analysis was duplicated, resulting in a total of two repetitions. The calculated average value was then utilized. Equation 5 was employed to determine the percentage of dyes adsorbed by Coconut Shell Biochar.

$$\% \text{ Removal} = \left[\frac{C_o - C_e}{C_o} \right] \times 100 \quad (5)$$

The solution's concentration during initial and equilibrium time was represented by C_o & C_e , and volume (v), adsorbent mass (m) also taken for experimental findings.

2.4. Isotherm studies

Indeed, adsorption isotherms play a crucial role in enhancing our understanding of the interaction between the adsorbate and the adsorbent. This knowledge is essential for maximizing the efficiency of adsorbent utilization. Drawing accurate conclusions from the equilibrium plot is crucial for optimizing the adsorption mechanism, as highlighted by Mustapha *et al.* in 2019. The resultant adsorption isotherm provides essential data for evaluating production in extensive industrial systems.

2.4.1. Langmuir isotherm

In the context of the Langmuir isotherm study, the analysis sheds light on the equilibrium established between the gas and adsorbent phases. This examination specifically centers on the concentrations of the fluid and solid components present within the adsorption process. Moreover, the research provides valuable understanding regarding the advancement of the adsorption mechanism. Based on the outcomes of the Langmuir isotherm analysis, it can be deduced that the adsorption process exhibits characteristics akin to a monolayer arrangement on the surface of the activated adsorbent (Haro *et al.*, 2021). This behavior is particularly evident under certain relative pressure conditions and within a heterogeneous environment. The fundamental idea behind this model is that the interaction between dye molecules and the coconut shell adsorbent is primarily driven by chemical

processes. The linear expression representing this isotherm analysis is captured in equation 6.

$$\frac{C_e}{q_e} = \frac{1}{K \cdot q_{max}} + \frac{C_e}{q_{max}} \quad (6)$$

Within this model, C_e symbolizes the dyes concentration, q_e signifies the quantity of dye molecules adsorbed, and the constants associated with capacity and intensity are denoted as K and q_{max} , correspondingly.

2.4.2. Freundlich isotherm

The alterations in adsorption concerning the quantity of adsorbed gas per unit mass of the activated charcoal adsorbent were explored under a precise temperature of 30°C. This investigation was conducted by observing changes in the system pressure. As reported by Malti *et al.* in 2022, this isotherm investigation has enabled the observation of multi-layer adsorption, attributed to the heterogeneous nature of the dye uptake process. The linear equation of the Freundlich isotherm model is represented by Equation 7.

$$\ln q_e = \ln k_f + \frac{1}{n} \ln C_e \quad (7)$$

The mass adsorption/gram of adsorbate was denoted by q_e in this study, whereas n represented the adsorption energy. K_f was utilized to signify the adsorption capacity, and C_e was used to denote the equilibrium concentration of the solution.

2.4.3. Temkin isotherm study

The linearity was reduced with increase in distance of layer of adsorbent molecules suggested by Temkin isotherm study. The isotherm equation resulting from Temkin research is expressed in Equation 8.

$$q_{eq} = \frac{RT}{b} \ln K_T + \frac{RT}{b} \ln C_e \quad (8)$$

Within the framework of Temkin isotherm studies, the determination of adsorbate equilibrium concentration (C_{eq}) involved the utilization of elements such as the equilibrium binding constant (K_T), temperature (T), the universal gas constant (R), and the adsorption heat constant (b).

2.4.4. Dubinin-Radushkevich (D-R) isotherm study

Adsorption does not need homogeneity or consistent sorption, and this study is similar to other isotherm models (Marah *et al.*, 2019). The linear form of D-R isotherm model was represented in Equation 9, can describes the dye adsorption nature.

$$\ln q_e = \ln x_m - \beta \epsilon^2 \quad (9)$$

q_e & x_m were used to identify the amount of pollutants uptake and capacity of adsorption at the time of equilibrium.

2.5. Kinetic Studies

The equilibrium studies were conducted by varying the dyes and their concentrations within the range of 20 to 100 mg/L. The conducted investigations were executed under a pH level of 10.0, employing 3 g/L of Coconut Shell

Biochar as the adsorbent. A 100 mL of dye solution underwent agitation within a rotary shaker, operating at a specified speed of 120 rpm for 60 minutes, maintaining at 30°C. Subsequently, the solution was filtered using a Whatman filter paper. The provided data on adsorption efficiency and scalability potential were then analyzed using the following adsorption kinetic models.

2.5.1. Pseudo – first order kinetic model

The Lagergren kinetic rate model for solid-liquid adsorption was formulated based on the concept of solid adsorption capacity. This kinetic model was developed by the researchers specifically to explore solute adsorption from the aqueous solution. This model assumes that the rate-limiting step of a chemical reaction or process is determined by the interaction of one reactant with a surface or a solid, and that the concentration of another reactant is in excess and remains essentially constant throughout the reaction (Pham *et al.*, 2021). To represent the pseudo-first-order kinetic model, Equation 10 was used.

$$\frac{dq_e}{dq_t} = k (q_e - q_t) \quad (10)$$

The total equilibrium quantity of adsorbed dyes at time 't' is derived by computing both q_e and q_t , with the rate constant represented as K.

2.5.2. Pseudo – Second order kinetic model

A second-order chemical adsorption process is used in this kinetic study, with the assumption that the adsorption rate is proportional to the square of the number of vacant sites (Venkatraman *et al.*, 2021). Equation 11 represents the expression for the pseudo-second-order kinetic equation.

$$\frac{t}{q_t} = \frac{1}{h} + \frac{1}{q_e} t \quad (11)$$

In this case, h represents the rate of adsorption during the stating time, and constant rate of adsorption was denoted by k.

2.5.3. Boyd kinetic model

The Boyd kinetic plot insights were used to investigate the adsorbent's most gradual adsorption stage. The Boyd kinetic equation is depicted as Equation 12.

$$\frac{q_t}{q_e} = 1 - \frac{6}{\Pi^2} \exp(-Bt) = F \quad (12)$$

q_t & q_e – The amount of dyes adsorbed at time 't' in the equilibrium is expressed in milligrams per gram (mg/g). The fraction of pollutants was denoted by F and the mathematical function was denoted by B. Equation 12 can be rearranged into linear form by taking natural logarithm represented in Equation 13.

$$Bt = -0.4977 - \ln(1 - F) \quad (13)$$

The calculated B_t values can be used to obtain the D_i values (Diffusion Co-efficient) represented in Equation 14.

$$B = \frac{\Pi^2 D_i}{r^2} \quad (14)$$

Using the above equation, the determination of both the ' D_i & r ' values was carried out. Additionally, the calculation of the adsorbent particle radius was conducted based on the assumptions formulated in sieve analysis.

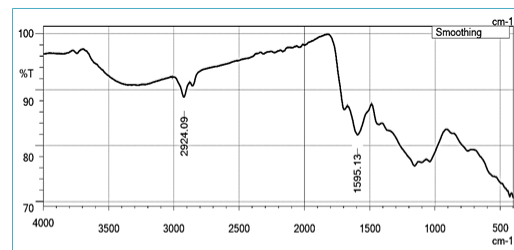
3. Results and discussion

3.1. Characterization of coconut shell biochar

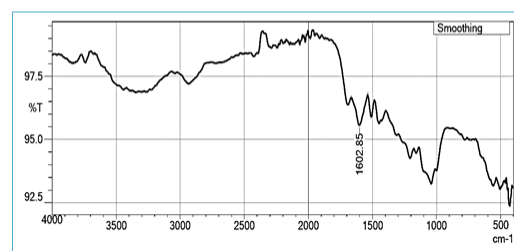
During batch adsorption investigations, the properties of the coconut shell biosorbent material are of paramount importance. To verify its capacity to remove specific pollutants, a comprehensive characterization study was carried out. This study involved multiple analyses, such as FTIR, SEM, EDX, and BET surface analysis. These analyses provided valuable insights into the structure and composition of the biosorbent material, shedding light on its potential as an efficient adsorbent for pollutant removal.

3.2. FTIR studies

FTIR analysis was performed to analyze the presence of various functional groups and elements for adsorbing the pollutants from aqueous medium. The FTIR spectra of untreated and activated coconut shell charcoal powder are shown in Figure 1(a) and (b), revealing a variety of functional groups. The analysis indicated a broad energy band extending from 3420 cm^{-1} to 2860 cm^{-1} , indicating the existence of -OH and -CH₂ functional groups. Various elements were discovered in the spectrum extending from 1800 to 1000 cm^{-1} , including the presence of water at 1620 cm^{-1} , aromatic compound vibrations between 1600 and 1400 cm^{-1} , -CH₂ bending vibrations between 1400 and 1380 cm^{-1} , and C-O stretching vibrations at 1080 cm^{-1} . The FTIR analysis revealed aromatic ring vibrations around 1000 cm^{-1} , attributed to -C-H bending, while lower frequency regions exhibited the -OH stretching phenomenon (Phuengphai *et al.*, 2021). These bandwidths and stretching vibrations further confirm the existence of various functional groups in the adsorbent, validating its capacity to effectively adsorb contaminants from the wastewater.



(a)



(b)

Figure 1. FTIR peaks of (a) coconut shell powder & (b) activated coconut shell powder

3.3. Pore distribution and surface area analysis

Figure 2 depicts the rate of nitrogen desorption from the coconut shell biochar adsorbent at -196°C using isotherm curves for both adsorption and desorption. This analysis of the curve was implemented to deduce the biochar adsorbent's surface area and pore size. The isotherm curve, categorized as type II, shows the occurrence of both micro and meso pores on the surface of the adsorbent. The initial curve demonstrates the existence of micro pores, while the subsequent curve signifies the presence of meso pores (Vera *et al.*, 2018). When compared to other commercially available activated carbons, the coconut shell biochar adsorbent demonstrated a substantially higher surface area of 3.74

Table 1. Size and pore characteristics of coconut shell biosorbent

Sl. No.	Adsorbent Property	Measured Unit	Measured value
1.	Adsorbent's Surface Area (BJH analysis)	m ² g ⁻¹	78.483
2.	Adsorbent's pore volume	cc g ⁻¹	0.212
3.	Adsorbent's Pore Radius	Å	44.373
4.	Adsorbent's Surface Area (BET analysis)	m ² g ⁻¹	3.74
5.	Adsorbent's pore diameter – Average value	nm	0.061

3.4. SEM analysis

SEM analysis was conducted to assess the surface features and imperfections of the adsorbent. In Figure 3a, the raw adsorbent's surface was examined, revealing the presence of numerous active sites. These active sites play a vital role in adsorbing azo dyes and other pollutants from the solution. Following that, the synthetic solution containing azo dyes was applied to the surface of the biochar adsorbent until saturation was obtained. The adsorbent's surface was contaminated by pollutants, as shown in Figure 3b, and the presence of active sites occupied by these pollutants was visible, resulting in a cloud-like visual aspect on the surface. Once the adsorbent's surface became saturated with pollutants, no further adsorption of azo dyes was observed, indicating the completion of the adsorption process. This observation is in line with the concept of adsorption saturation (Hong *et al.*, 2020). Additionally, the presence of pollutants in both the inner and outer pores of the biochar's surface further supports the occurrence of the adsorption process.

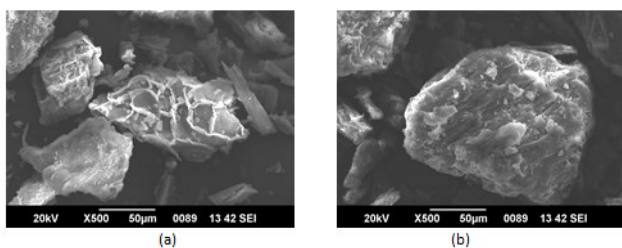


Figure 3. Scanning electron microscope analysis of coconut shell biochar (a) raw & (b) dye molecules loaded respectively

3.5. EDX analysis

The kinds of contaminants absorbed by the biochar adsorbent were determined using EDX analysis. Figure 4

m²/g. Table 1 clearly summarizes the relevant properties derived from the linear curves.

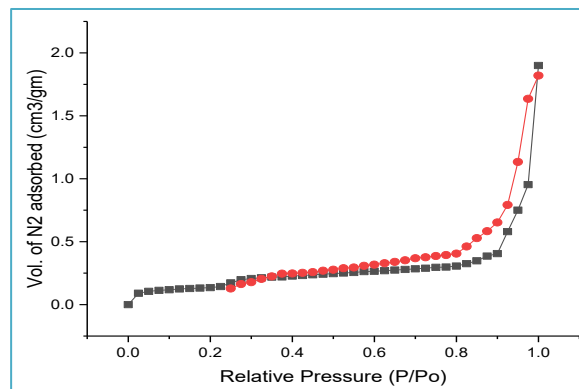


Figure 2. Surface area analysis of coconut shell biosorbent

(a) displays the EDX plot of the raw biochar adsorbent before the uptake of pollutants, revealing the presence comprising a range of organic and inorganic constituents as potassium, calcium, carbon, and aluminum. On the other hand, Figure 4 (b) shows the EDX plot of the biochar adsorbent after adsorbing azo dyes. In this image, elements including magnesium, calcium, iron, aluminum and silica were noticed on the surface of the adsorbent, resulting from the physical and chemical interactions during the synthesis of the adsorbent material (Boubaker *et al.*, 2021). These findings suggest that the biochar adsorbent has the capability to effectively adsorb pollutants from synthetic solutions, making it a promising material for pollutant removal applications.

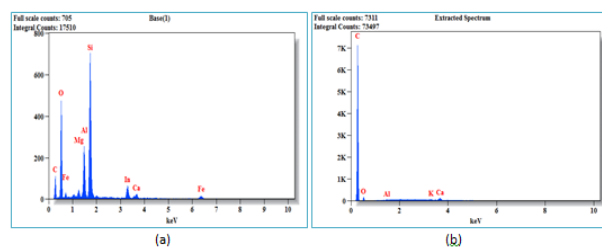


Figure 4. EDX plots of biosorbent material, (a) before and (b) after taking the pollutants

3.6. Batch adsorption studies

3.6.1. Impact of pH

In the investigation of dye adsorption, the impact of pH on the process was explored using a synthetic solution with pH values ranging from 2.0 to 12.0. During a 60-minute contact period, the concentration of each dye in the solution was maintained at a constant 20 mg/L, while the dosage of the coconut shell biosorbent was held steady at 1 g/L. The study aimed to elucidate the influence of pH variations on the adsorption behavior. Figure 5 depicts the

relationship of adsorption of dyes and the solution's pH. As the pH of the solution increased, the adsorption capacity also showed an increase. This can be attributed to the presence of charged adsorbent sites with a positive nature, leading to interactions with the coconut shell biosorbent. At higher pH levels, the adsorbent surface becomes more positively charged, resulting in more efficient removal of dyes from the solution (Bayuo *et al.*, 2019). The results suggest that the solution's pH plays a significant role in enhancing the adsorption process, particularly at higher pH values where the positive charge on the adsorbent surface promotes rapid elimination of dyes. This information is vital for optimizing the adsorption process and designing effective water treatment strategies using coconut shell biosorbent.

As depicted in Figure 5, the adsorbent exhibited the highest dye uptake at a pH of 10.0, indicating its optimal performance. However, beyond this pH, there was a gradual decrease in dye removal efficiency. This decline can be attributed to the precipitation of metal hydroxides at higher pH values, resulting in reduced availability of dyes for adsorption (Priya *et al.*, 2022). At the optimum pH of 10.0, the coconut shell activated carbon demonstrated exceptional adsorption capacities, effectively removing 87.12% of CV ions and 92.28% of MB dyes from the solution. This underscores the remarkable adsorption performance of coconut shell activated carbon for these specific dyes, making it an excellent adsorbent for achieving optimal pollutant removal. To maximize the efficiency of coconut shell activated carbon as an effective adsorbent for the removal of CV and MB dyes from contaminated water sources, it is crucial to maintain the pH within the appropriate range.

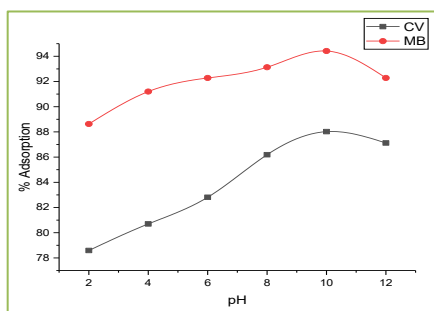


Figure 5. Changes in adsorption efficiency by altering solution's pH

3.6.2. Impact of coconut shell biochar dose

As depicted in Figure 6, the concentration of coconut shell biochar dose has a significant impact on the adsorption of pollutants in the synthetic solution. Within the scope of the batch mode examination, a spectrum of adsorbent dosage levels was explored, ranging from 1 to 3.5 g/L. Throughout this spectrum, the pH of the solution was consistently maintained at 10.0, while the synthetic solution remained at a steadfast concentration of 20 mg/L, and the contact period persisted for 60 minutes. The findings distinctly illustrate that the absorption of dyes from the synthetic solution escalates as the dosage of coconut shell biochar rises. The peak adsorption efficiency was observed when using a dosage of 3 g/L.

However, exceeding this dosage threshold, the concentration gradient had minimal effects on dye absorption from aqueous solutions (Su *et al.*, 2021). This suggests that a dosage level of 3 g/L is adequate to achieve the maximum adsorption efficiency. These findings underscore the importance of selecting an appropriate dosage level of neem leaf biochar to optimize pollutant removal from contaminated water sources. The dosage level of 3 g/L was found to be the most effective in this study, providing valuable insights for the practical application of neem leaf biochar as an adsorbent in water treatment processes. By utilizing the appropriate dosage, the adsorption capacity of neem leaf biochar can be maximized, ensuring efficient and cost-effective pollutant removal from water sources. The enhanced dyes uptake with an increase in biochar dose can be attributed to the greater availability of free active surface area for adsorbing the dye molecules (Usha *et al.*, 2021). The study revealed that a dosage of 3 g/L of coconut shell biochar was particularly effective, leading to the adsorption of 80.48% of CV and 70.28% of MB dyes from the aqueous solutions. This indicates that increasing the dosage of coconut shell biochar significantly improves its adsorption capacity, resulting in higher pollutant removal efficiency. The optimal dosage of 3 g/L strikes a good balance between the availability of surface area and the efficiency of pollutant adsorption, making it a favorable choice for efficient water purification applications. By utilizing the appropriate dosage of coconut shell biochar, water treatment processes can be optimized to effectively remove pollutants from contaminated water sources.

3.6.3. Impact of contact time

In this study, the contact time between the pollutants and the adsorbent material was investigated to understand its influence on the adsorption process. The concentration of dyes within the synthetic solutions underwent alteration of 20-100 mg/L, whereas the contact time was modulated across a span of 10 to 80 minutes. The pH of the solution was maintained at 10.0, and the biochar dosage was set at 3 g/L. Referring to Figure 7 (a) & (b), it is evident that the amount of dye uptake was initially, the process exhibited rapid kinetics owing to the presence of abundant active and unoccupied sites within the adsorbent material. As the procedure progressed, the adsorption eventually reached a point of saturation within the mesopores of the biochar (Uduakobong *et al.*, 2020). The figure demonstrates that the maximum efficiency was achieved within 60 minutes of contact time, indicating that this duration is sufficient to achieve optimal pollutant removal. This information is valuable for designing efficient water treatment processes using coconut shell biochar as an effective adsorbent for dye removal from contaminated water sources. Beyond 60 minutes, there was no significant improvement in adsorption efficiency, suggesting that prolonged contact time may not yield further benefits in terms of pollutant uptake. As the adsorption process progresses, factors like surface repulsion, mass transfer limitations, and energy barriers for pore penetration contribute to a constant quantity of

dye uptake by the adsorbent, resulting in steady adsorption efficiency (Saruchia *et al.*, 2019). The study demonstrated that the maximum efficiency of 86.34% for CV and 89.83% for MB dyes was achieved with an optimum contact time of 60 minutes and a dye concentration of 20 mg/L. These findings highlight the importance of optimizing contact time for effective dye removal using coconut shell biochar as an adsorbent in water treatment processes.

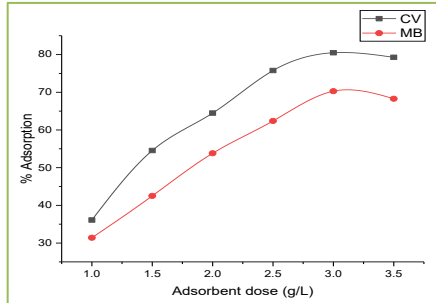


Figure 6. Adsorption efficiency changes according to biochar dosage

3.6.4. Impact of dye concentration

The presence of high concentrations of dyes in aqueous solutions not only poses a threat to the environment but also affects the adsorption capacity of the activated adsorbent material. This study encompassed a range of dye concentrations from 20 to 100 mg/L, aiming to assess their influence on adsorption efficiency. Throughout the investigation, a solution with a pH of 10.0, a coconut shell biochar dosage of 3 g/L, and a contact period of 60 minutes were maintained. Observing Figure 8, it becomes evident that the adsorption of dyes transpired swiftly at lower concentrations. However, as the dye concentration in the solution gradually escalated, the rate of dye uptake exhibited a corresponding decline. At lower concentrations, the adsorption process was rapid due to the abundance of large active sites on the adsorbent surface (Malima *et al.*, 2021). As the dyes were absorbed, the adsorbent reached its saturation point in the mesopores. In this batch study, a concentrated dye solution of 20 mg/L showed achieving a notable level of adsorption efficiency through the utilization of coconut shell biosorbent. At lower concentrations, the activated adsorbent material managed to adsorb as much as 88.45% of CV and 90.29% of MB dyes. The swift absorption of dyes at lower concentrations suggests that the adsorbent has not yet reached its saturation point, and there are still vacant active sites available for further adsorption. This finding highlights the potential of coconut shell biosorbent as a proficient and effective option for eliminating dyes from polluted water sources, especially when dealing with lower dye concentrations (Eleryan *et al.*, 2022).

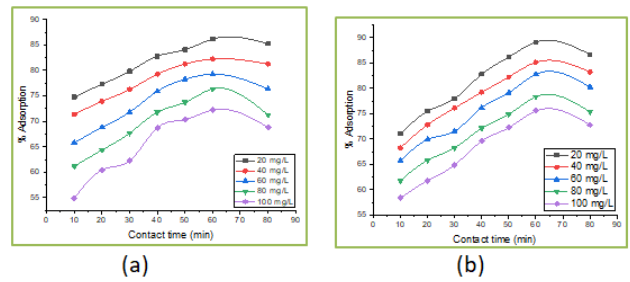


Figure 7. Adsorption efficiency changes with contact time for (a) CV and (b) MB dyes

3.6.5. Impact of temperature

The effect of temperature on the adsorption of azo dyes using coconut shell biochar was investigated by conducting experimental investigations at different temperatures, ranging from 20 to 60°C, as depicted in Figure 9 (a) & (b) for CV and MB dyes. Temperature is a crucial parameter in adsorption studies that can significantly impact the adsorption process. Upon analyzing the temperature study plots, it was observed that the maximum amount of azo dye removal occurred at 20°C. However, as the temperature was gradually increased up to 60°C, there was a noticeable decrease in the uptake of azo dyes by the coconut shell biochar. This reduction in dye uptake at higher temperatures can be attributed to the exothermic nature of the adsorption process (Fideles *et al.*, 2019). The increase in temperature may lead to a decrease in the available active sites on the adsorbent surface, thereby reducing the adsorption capacity for the azo dyes. As a result, the efficiency of dye adsorption by the coconut shell biochar decreased with increasing temperature. These findings highlight the importance of considering temperature as a critical factor in optimizing the adsorption process using coconut shell biochar for the removal of azo dyes from water sources (Sasireka *et al.*, 2021).

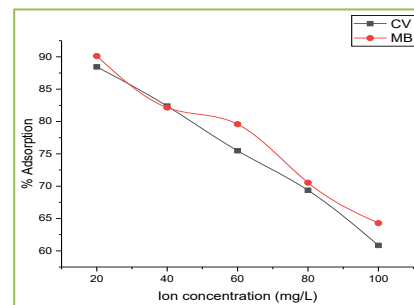


Figure 8. Adsorption effectiveness changes due to dye concentration changes

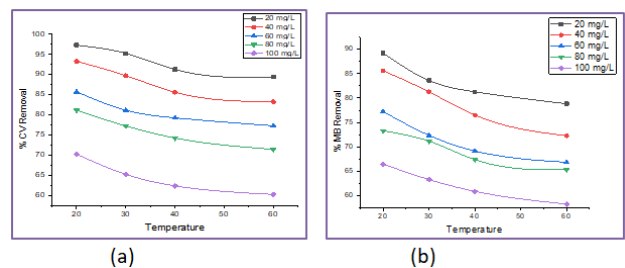


Figure 9. Changes in adsorption efficiency by varying solution's temperature for (a) CV& (b) MB dyes

3.7. Isotherm studies

3.7.1. Langmuir isotherm

The Langmuir isotherm coefficients (k and q_{\max}) were calculated by analyzing the inclination and deviation data retrieved from the C_e/q_e versus C_e linear isotherm plot. Figure 10 showcases the linear diagrams derived from the Langmuir isotherm analysis, while the values of the constants (k , q_{\max}) are ascertained and exhibited in Table 2. The regression values obtained at a temperature of 30°C, which are higher than the average values ($R^2 > 0.95$), underscore the suitability of this isotherm model in elucidating the adsorption mechanism. Furthermore, the computed separation factor (R_L) values for a dye concentration of 20 mg/L were found to span the interval from 0 to 1. This affirmation solidifies the occurrence of a monolayer adsorption process, which can transpire through either physical or chemical means, validating the effectiveness of the adsorption process. R_L values less than 1 suggest favorable adsorption conditions, indicating that the adsorption of dyes onto the adsorbent is favorable and efficient at this concentration (Wang *et al.*, 2020). The successful application of the Langmuir isotherm model and the favorable R_L values for the adsorption process at 20 mg/L concentration highlight the potential of this adsorbent for the removal of dyes from aqueous solutions. These findings are valuable for optimizing the adsorption process and designing efficient water treatment strategies using the coconut shell adsorbent.

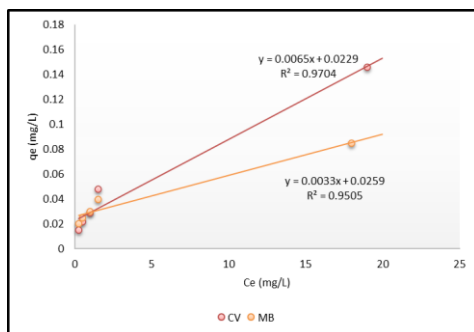


Figure 10. Langmuir isotherm plot for the adsorption of dyes using coconut shell biochar

3.7.2. Freundlich isotherm

The Freundlich isotherm is a versatile model that permits the potential for multilayer adsorption to occur, encompassing both physical and chemical mechanisms. Figure 11 illustrates the linear graphs of $\ln q_e$ against $\ln C_e$ at a temperature of 30°C, while the corresponding isotherm constants K_f and n values are detailed in Table 2. The value of constant n , which ranges from 1 to 10, suggests that the adsorption of dyes by coconut shell biochar powder may predominantly involve physical adsorption (Wang *et al.*, 2022). Interestingly, the experimental data exhibits good conformity with both the Langmuir and Freundlich isotherm models, indicating that either model can effectively describe the adsorption process. The computed regression values (R^2) from the linear plots also demonstrate strong concurrence with both isotherm models, further highlighting the usefulness and applicability of these models in analyzing the

adsorption behavior of dyes using coconut shell biochar. The ability of the Freundlich isotherm to account for multilayer adsorption in both physical and chemical modes make it a valuable tool in understanding the adsorption process and optimizing the use of coconut shell biochar as an adsorbent for dye removal in water treatment applications (Dada *et al.*, 2021).

3.7.3. Temkin isotherm

The bio-adsorbent demonstrated an impressive ability to adsorb dyes from aqueous solutions. Adsorption isotherm studies were conducted to characterize the adsorbent material and ascertain various parameters including pore size, pore volume, and specific surface area. To gain further insights into the adsorbent's characteristics, the adsorption process of dyes (CV and MB) by coconut shell biochar was investigated using the Temkin isotherm model. Figure 12 depicts the Temkin plots (q_e vs. C_e) for dye adsorption, from which the kinetic constants (K_T and b) were determined. At a temperature of 30°C, the adsorption process demonstrated a strong alignment with the Temkin isotherm model, as indicated by the high R^2 values presented in Table 2. The fitting process with the Temkin isotherm model allowed for the evaluation of binding energies and the uniform distribution of adsorption sites, providing valuable information about the interactions between the adsorbent and dye molecules (Tovar *et al.*, 2021). Furthermore, the substantial amount of dye adsorption suggested that a monolayer adsorption process occurs during the connections among the coconut shell biochar and the dye molecules. This finding underscores the remarkable effectiveness of coconut shell biochar as an adsorbent material for the removal of dyes from water sources. Given its promising performance, coconut shell biochar holds great potential for practical applications in water treatment processes, contributing to the mitigation of dye contamination in aquatic environments (Panda *et al.*, 2020).

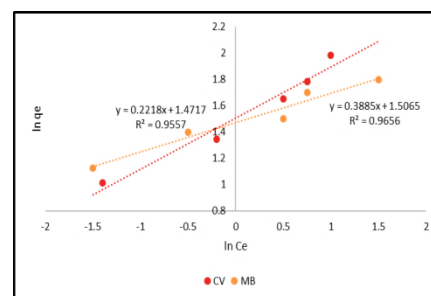


Figure 11. Freundlich isotherm plot for the adsorption of dyes using coconut shell biochar

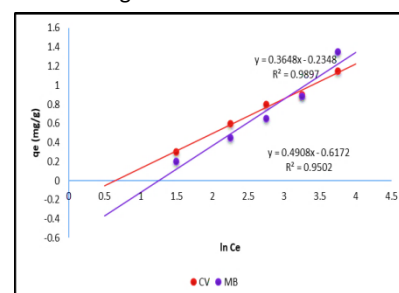


Figure 12. Temkin isotherm plot for the adsorption of dyes using coconut shell biochar

3.7.4. D-R isotherm

The adsorption process of CV and MB dyes by coconut shell biochar was explored utilizing the D-R isotherm study to classify the behavior of the biosorbent. Figure 13 depicts the D-R isotherm plots (ln qe versus ϵ^2) for CV and MB dyes, while Table 2 lists the relevant constants. The D-R isotherm investigation was carried out at a constant temperature of 30°C, after which the regression coefficient (R^2) values were computed. The R^2 values obtained for both CV and MB dyes were found to be greater than 0.95, indicating that the D-R isotherm model provided a good fit for the adsorption process. Furthermore, the R^2 values obtained from the Langmuir, Freundlich, and Temkin isotherm plots were compared to determine the best fit for the isotherm study. The results showed that for both CV and MB dyes, the Freundlich isotherm provided the best fit, followed by the Langmuir, Temkin, and D-R isotherms. This indicates that the Freundlich isotherm model is more suitable for describing

the adsorption process of CV and MB dyes by coconut shell biochar, suggesting a multilayer adsorption with heterogeneous characteristics (Nathan *et al.*, 2021). However, the agreement of R^2 values with the Langmuir, Temkin, and D-R isotherms also indicates that these models can adequately describe the adsorption process with monolayer and heterogeneous adsorption behavior.

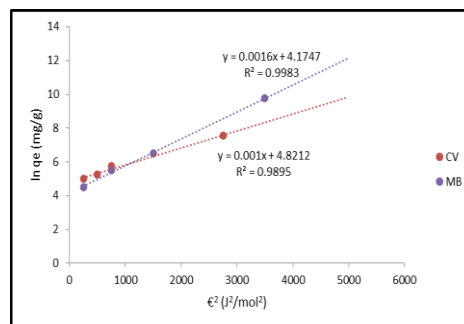


Figure 13. D-R isotherm plot for dye adsorption using coconut shell biochar

Table 2. Adsorption isotherm constants for dye molecules

Type of study	Parameters	Units	CV	MB
Langmuir	q_{max}	mg/g	11.293	9.348
	K_L	1/mol	0.419	0.501
	R^2	-	0.9704	0.9505
Freundlich	K_f	L/g	3.192	2.947
	n	-	3.029	2.847
	R^2	-	0.9557	0.9656
Temkin	K_T	L/Mol	1.27×10^7	1.51×10^4
	$b \times 10^{-6}$	J g mol ⁻²	28.4	23.8
	R^2	-	0.9897	0.9502
D-R	$X_m \times 10^{-3}$	(mol/g)	4.51	3.76
	ϵ	KJ/mol	10.98	10.31
	R^2	-	0.9983	0.9895

3.8. Kinetic studies

The kinetics of CV and MB dye adsorption using coconut shell biochar were investigated through various models, including pseudo-first-order, pseudo-second-order, and Boyd kinetic models. The experiments were conducted at different time intervals to determine the dominant mechanism of adsorption, whether it involves physical interactions or chemical bonding between the dye molecules and the biochar surface. By comparing the results from these kinetic studies, valuable insights can be gained regarding the nature of the adsorption process and the dominant mechanisms driving the CV and MB dye adsorption on coconut shell biochar.

3.8.1. Pseudo first order study

Figure 14 depicts the kinetic plot generated from the pseudo-first-order study [(qe - q) vs. t], whereas Table 3 has the appropriate constants for this kinetic model. The study included varying the quantities of CV and MB dyes in the synthetic solution from 20 to 100 mg/L to see how they affected the adsorption process. The Lagergren kinetic plot produced a regression value greater than 0.95, indicating that this kinetic research was well aligned with the adsorption process. Table 3 shows how the constant 'k' was calculated and reported. The model predicts that

the adsorption process reaches a saturation threshold beyond which no further absorption of dye molecules occurs, based on the regression data. The pseudo-first-order kinetic model provided valuable insights into the adsorption behavior of CV and MB dyes using the coconut shell biochar material (Mwandira *et al.*, 2020).

3.8.2. Pseudo second order study

The concentration of azo dyes and the response of the manufactured biochar adsorbent during the adsorption process were examined using second-order experiments. To test the application of second-order kinetics, regression values were obtained using the linear plots in this investigation, as shown in Figure 15. The obtained regression values from each linear plot were found to be very high, indicating a good fit with the batch studies. This suggests that the adsorption of CV and MB dyes by the coconut shell adsorbent can be attributed to either physical or chemical mechanisms, as supported by the applicability of the second-order kinetic model. Consequently, the prepared biochar adsorbent shows promising performance for the targeted adsorption of azo dyes through a chemisorption process (Ma *et al.*, 2022).

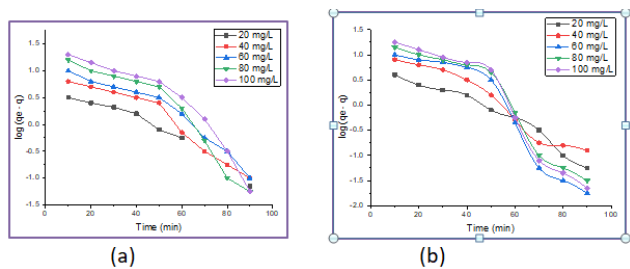


Figure 14. Pseudo first order plots for the adsorption of (a) CV & (b) MB dye molecules using coconut shell biosorbent

3.8.3. Boyd kinetic study

Figure 16 displays linear graphs depicting Bt vs. t , revealing the linearity of the Boyd kinetic model. Nevertheless, the plots do not originate from the origin, implying the presence of external film diffusion during the adsorption of dyes by coconut shell biochar. The Boyd

kinetic constants (Di and B) were derived by analyzing the slope and intercept of the linear plots and are shown in Table 3. Despite the linearity of the plots, the regression results (R^2) for this kinetic model were found to be low, indicating that the Boyd kinetic model is not applicable in this batch study for describing the adsorption of dyes by coconut shell biochar.

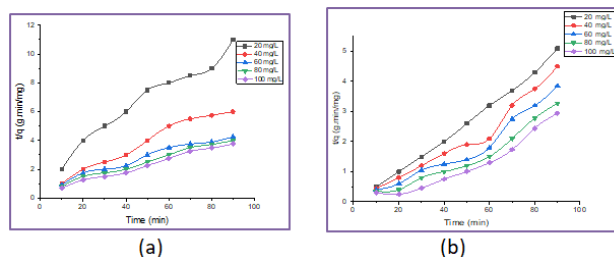


Figure 15. Pseudo second order plots for the adsorption of (a) CV & (b) MB dye molecules using coconut shell biosorbent

Table 3. Adsorption kinetic constants for dye removal using coconut shell biosorbent

S. No.	Name of the dye	Conc. (mg/L)	Pseudo First order			Pseudo Second order				Boyd		
			K (min ⁻¹)	q _{e,cal} (mg/g)	R ²	K (g/mg.min) × 10 ⁻³	q _{e,cal} (mg/g)	h (mg/g.min)	R ²	B	D _i (x 10 ⁻³ m ² /s)	R ²
1.	CV	20	0.034	2.64	0.95	16.69	2.15	0.10	0.96	0.034	5.472	0.915
2.		40	0.043	7.02	0.93	5.73	5.19	0.18	0.98	0.044	7.340	0.973
3.		60	0.041	10.00	0.93	3.34	8.30	0.22	0.98	0.043	7.621	0.963
4.		80	0.039	11.36	0.94	5.07	10.75	0.26	0.98	0.039	6.856	0.914
5.		100	0.048	17.47	0.92	2.00	12.91	0.29	0.97	0.049	8.725	0.982
6.	MB	20	0.046	3.68	0.91	12.62	2.70	0.10	0.97	0.046	7.678	0.943
7.		40	0.041	6.54	0.93	5.32	5.47	0.12	0.98	0.041	6.294	0.983
8.		60	0.043	9.95	0.92	3.56	8.60	0.23	0.98	0.045	7.959	0.924
9.		80	0.046	12.38	0.94	2.77	10.10	0.28	0.97	0.046	7.678	0.983
10.		100	0.052	20.55	0.92	2.30	11.56	0.31	0.98	0.053	8.590	0.941

3.8.4. Thermodynamic studies

The thermodynamic plots ($\log K_c$ vs. $1/T$) shown in Figure 17 provide insights into the adsorption process of CV and MB dyes at different concentrations (ranging from 25 to 150 mg/L) using coconut shell biochar. From these plots, the slope and intercept values were determined, representing the change in enthalpy (ΔH°) and change in entropy (ΔS°), respectively. These thermodynamic parameters are crucial in understanding the energetics of the adsorption process (Table 4). The negative ΔH° values indicate that the adsorption process is exothermic, meaning that heat is released during the adsorption of CV and MB dyes onto the coconut shell biochar. This exothermic nature of the process suggests that the adsorption is favored at lower temperatures. Additionally, the negative ΔG° values imply that the adsorption is

spontaneous and thermodynamically favorable, as the system tends to move towards lower energy states. Furthermore, the positive ΔS° values indicate an increase in uncertainty or randomness during the adsorption process (Silva *et al.*, 2015). This suggests that the adsorption of CV and MB dyes onto the biochar surface results in an increase in disorder or entropy within the system. This rise in entropy contributes to the adsorption process's favorable character. Overall, the thermodynamic analysis confirms that the adsorption of CV and MB dyes using coconut shell biochar is spontaneous, exothermic, and associated with increased entropy. This information is valuable in understanding the energetics of the adsorption process and optimizing the conditions for efficient removal of dyes from aqueous solutions using coconut shell biochar as an adsorbent.

Table 4. Dye molecules adsorption using coconut shell powder: Thermodynamic constants

CV – Initial Concentration	ΔH° (KJ/mol)	ΔS° (J/mol)	ΔG° (kJ/mol)			
			15°C	30°C	45°C	60°C
20	-83.38	222.52	-15.90	-10.82	-9.24	-8.24
40	-42.73	96.87	-11.31	-8.98	-7.45	-7.32
60	-26.45	61.28	-8.60	-7.45	-6.58	-6.15
80	-19.64	41.29	-6.69	-6.72	-6.19	-5.93
100	-16.82	32.35	-6.24	-6.12	-5.68	-5.28

MB – Initial Concentration						
20	-56.24	143.77	-13.30	-11.15	-8.93	-8.13
40	-31.69	72.86	-9.02	-8.80	-7.47	-6.69
60	-26.44	56.98	-8.12	-6.90	-6.64	-5.51
80	-19.89	39.31	-7.62	-6.09	-5.38	-5.20
100	-15.49	21.83	-6.63	-5.44	-4.92	-4.69

3.9. Desorption studies of spent adsorbent

The proper disposal of used adsorbent poses a significant challenge in the adsorption process and can lead to significant environmental contamination. To address this issue and enhance the cost-effectiveness of the adsorption process, the regeneration of used adsorbent becomes crucial. To recover the dyes, desorption investigations were performed utilizing concentrated hydrochloric acid at varying concentrations, ranging from 0.1N to 0.4N. During the desorption process, the retrieval of dyes from the exhausted adsorbent exhibited swift advancement primarily in the initial stages. However, the retrieval of dyes exhibited a substantial decline until reaching a hydrochloric acid concentration of 0.3N, after which it stabilized (Mahendra Kumar *et al.*, 2019). These findings indicate that 0.3N hydrochloric acid concentration yielded the optimal dye recovery, with no further improvement observed at higher concentrations. The investigation successfully reclaimed approximately 87.31% of CV and 81.28% of MB dyes from the surface of coconut shell biochar through the use of 0.3N hydrochloric acid. The subsequent utilization of the recovered dyes in various experimental procedures showcased the efficacy of dye recovery through desorption using hydrochloric acid, highlighting its potential for diverse applications.

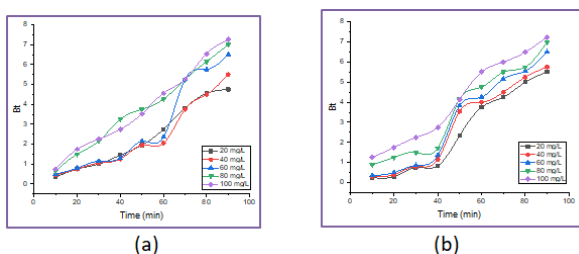


Figure 16. Boyd kinetic plots for the adsorption of (a) CV & (b) MB dye molecules using coconut shell biosorbent

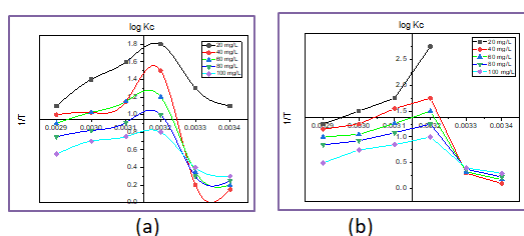


Figure 17. Thermodynamic plots of (a) CV & (b) MB dyes adsorption using coconut shell biochar

4. Conclusion

Batch mode adsorption tests were conducted to assess the efficacy of coconut shell biosorbent in the removal of crystal violet and methylene blue dyes from wastewater. The experiments were performed at room temperature (25°C), and a comprehensive set of isothermal tests,

including Langmuir, Freundlich, Temkin, and Dubinin-Radushkevich (D-R) models, indicated a heterogeneous multilayer adsorption process. Additionally, pseudo-first-order and pseudo-second-order kinetic experiments, along with Boyd kinetic studies, provided evidence supporting the hypothesis that the uptake of dye molecules by the coconut shell adsorbent occurred through a chemical adsorption process. Thermodynamic analyses indicated that the dye adsorption process was exothermic. In the context of desorption studies, the application of concentrated hydrochloric acid led to the efficient recovery of 89.74% of crystal violet and 82.32% of methylene blue dye molecules, further highlighting the potential of this approach for effective dye recovery from the adsorbent. The findings underscore the significant potential of coconut shell biosorbent as an effective solution for the removal of concentrated colors from wastewater. Additionally, the biosorbent's demonstrated capability for desorption and successful recovery of dye molecules further enhances its suitability for practical applications in wastewater treatment processes.

References

- Bayuo J, Pelig-Ba K.B., Abukari M.A. (2019). Adsorptive removal of chromium(VI) from aqueous solution unto groundnut shell, *Applied water science*, **9**, 107, <https://doi.org/10.1007/s13201-019-0987-8>
- Bich Ngoc Pham, Jin-Kyu Kang, Chang-Gu Lee, and Seong-Jik Park (2021). Removal of Heavy Metals (Cd^{2+} , Cu^{2+} , Ni^{2+} , Pb^{2+}) from Aqueous Solution Using *Hizikia fusiformis* as an Algae-Based Bioadsorbent, *Applied Sciences*, **11(18)**, 8604, <https://doi.org/10.3390/app11188604>
- Boubaker H., Arfi R.B., Mougin K., Vaultot C., Hajj S., Kunneman P., Schrodj G. and Ghorbal A. (2021) New optimization approach for successive cationic and anionic dyes uptake using reed-based beads, *Journal of Cleaner Production*, **307**, 127218, <https://doi.org/10.1016/j.jclepro.2021.127218>
- Dada A.O., Adekola F.A., Odeunmi E.O., Ogunlaja A.S. and Bello O.S. (2021). Two–three parameters isotherm modeling, kinetics with statistical validity, desorption and thermodynamic studies of adsorption of Cu (II) ions onto zerovalent iron nanoparticles, *Scientific Reports*, **11**, 16454, <https://doi.org/10.1038/s41598-021-95090-8>
- Edet U.A. and Ifelegegu A.O. (2020). Kinetics, Isotherms, and Thermodynamic Modeling of the Adsorption of Phosphates from Model Wastewater Using Recycled Brick Waste, *Processes*, **8**, 665, <https://doi.org/10.3390/pr8060665>
- El Malti W., Hijazi A., Abou Khalil Z., Yaghi Z., Medlej M.K. and Reda M. (2022). Comparative study of the elimination of copper, cadmium, and methylene blue from water by adsorption on the citrus *Sinensis* peel and its activated carbon, *RSC Advances*, **12**, 10186, <https://doi.org/10.1039/D1RA08997H>

- Eleryan A., Aigbe U.O., Ukhurebor K.E., Onyancha R.B., Eldeeb T.M., El-Nemr M.A., Hassaan M.A., Ragab S., Osibote O.A., Kusuma H.S., Darmokoeseoemo H. and El Nemr A. (2022). Copper(II) ion removal by chemically and physically modified sawdust biochar, *Biomass Conversion and Biorefinery*, <https://doi.org/10.1007/s13399-022-02918-y>
- Fideles R.A., Teodoro F.S., Xavier A.L.P., Adarme O.F.H., Gil L.F. and Gurgel L.V.A. (2019). Trimellitated sugarcane bagasse: A versatile adsorbent for removal of cationic dyes from aqueous solution. Part II: Batch and continuous adsorption in a bicomponent system, *Journal of Colloid and Interface Science*, **552(15)**, 752–763, <https://doi.org/10.1016/j.jcis.2019.05.089>
- Haro N.K., Dávila I.V.J., Nunes K.G.P., de Franco M.A.E., Marcilio R.M. and Féris L.A. (2021). Kinetic, equilibrium and thermodynamic studies of the adsorption of paracetamol in activated carbon in batch model and fixed-bed column, **11 (38)**, <https://doi.org/10.1007/s13201-020-01346-5>
- Hong J., Xie J., Mirshahghassemi S., Lead J. (2020). Metal (Cu, Cr, Ni, Pb) removal from environmentally relevant waters using polyvinylpyrrolidone – coated magnetic nanoparticles, *RSC advances*, **10**, 3266–3276, Doi: <https://doi.org/10.1039/C9RA10104G>
- Khan T.A., Noumana Md., Dua D., Khan S.A. and Alharthi S.S. (2022). Adsorptive scavenging of cationic dyes from aquatic phase by H₃PO₄ activated Indian jujube (*Ziziphus mauritiana*) seeds based activated carbon: Isotherm, kinetics, and thermodynamic study, *Journal of Saudi Chemical Society*, **26 (2)**, 101417, <https://doi.org/10.1016/j.jscs.2021.101417>
- Kumar M., Singh A.K., Sikardhar M. (2019). Biosorption of Hg (II) from aqueous solution using algal biomass: Kinetics and isotherm studies, *Heliyon*, **6(1)**, e03321, <https://doi.org/10.1016/j.heliyon.2020.e03321>
- Kumari U., Mishra A., Siddiqi H. and Meikap B.C. (2021). Effective defluoridation of industrial wastewater by using acid modified alumina in fixed-bed adsorption column: Experimental and breakthrough curves analysis, *Journal of Cleaner Production*, **279**, 123645, <https://doi.org/10.1016/j.jclepro.2020.123645>
- Ma X., Liu Y., Zhang Q., Sun S., Zhou X and Xu Y. (2022). A novel natural lignocellulosic biosorbent of sunflower stem-pith for textile cationic dyes adsorption, *Journal of Cleaner Production*, **331**, 129878, <https://doi.org/10.1016/j.jclepro.2021.129878>
- Malima N., Owonubi S.J., Lugwisha E.H. and Mwakaboko A.S. (2021). Thermodynamic, isothermal and kinetic studies of heavy metals adsorption by chemically modified Tanzanian Malangali kaolin clay. *International Journal of Environmental Science and Technology*, **18 (10)**, 1–16. <http://dx.doi.org/10.1007/s13762-020-03078-0>
- Marah W. Khalid and Sami D. Salman (2019). Adsorption of Heavy Metals from Aqueous Solution onto Sawdust Activated Carbon, *Al-Khwarizmi Engineering Journal*, **15(3)**, 60–69, <https://doi.org/10.22153/kej.2019.04.001>
- Mustapha S., Shuaib D.T., Ndamitso M.M. *et al.* (2019). Adsorption isotherm, kinetic and thermodynamic studies for the removal of Pb(II), Cd(II), Zn(II) and Cu(II) ions from aqueous solutions using Albizia lebeck pods, *Applied water science*, **9**, 142, <https://doi.org/10.1007/s13201-019-1021-x>
- Mwandira W., Nakashima K., Kawasaki S., Arabelo A., Banda K., Nyambe I., Chirwa M., Ito M., Sato T., Igarashi T., Nakata H., Nakayama S. and Ishizuka M. (2020). Biosorption of Pb (II) and Zn (II) from aqueous solution by *Oceanobacillus profundus* isolated from an abandoned mine, *Scientific Reports*, **10**, 21189, <https://doi.org/10.1038/s41598-020-78187-4>
- Nathan R.J., Martin C.E., Barr D. and Rosengren R.J. (2021). Simultaneous removal of heavy metals from drinking water by banana, orange and potato peel beads: a study of biosorption kinetics, *Applied Water Science*, **11**, 116, <https://doi.org/10.1007/s13201-021-01457-7>
- Panda L., Jena S.K., Rath S.S. and Misra P.K. (2020). Heavy metal removal from water by adsorption using a low-cost geopolymer, *Environmental Science and Pollution Research*, **27**, 24284–24298, <https://doi.org/10.1007/s11356-020-08482-0>
- Phuengphai P., Singjanusong T., Kheangkun N. and Wattanakornsiri A. (2021). Removal of copper (II) from aqueous solution using chemically modified fruit peels as efficient low-cost biosorbents, *Water Science and Engineering*, **14(4)**, 286–294, <http://dx.doi.org/10.1016/j.wse.2021.08.003>
- Priya A.K., Yogeshwaran V., Rajendran S., Hoang T.K.A., Soto-Moscoco M., Ghfar A.A. and Bathula C. (2022). Investigation of mechanism of heavy metals (Cr⁶⁺, Pb₂₊ & Zn²⁺) adsorption from aqueous medium using rice husk ash: Kinetic and thermodynamic approach, *Chemosphere*, **286**, 131796, <https://doi.org/10.1016/j.chemosphere.2021.131796>
- Regti1 A., Laamari M.R., Stiriba S.E. and El Haddad M. (2017). The potential use of activated carbon prepared from *Ziziphus* species for removing dyes from waste waters, *Applied Water Science*, **7**, 4099–4108, Doi: <https://doi.org/10.1007/s13201-017-0567-8>
- Rincón-Silva N.G., Moreno-Piraján J.C. and Giraldo L.G. (2015). Thermodynamic Study of Adsorption of Phenol, 4-Chlorophenol, and 4-Nitrophenol on Activated Carbon Obtained from Eucalyptus Seed, ID 569403. <https://doi.org/10.1155/2015/569403>
- Saruchia and Kumar V. (2019). Adsorption kinetics and isotherms for the removal of rhodamine B dye and Pb⁺² ions from aqueous solutions by a hybrid ion-exchanger, *Arabian Journal of Chemistry*, **12(3)**, 316–329. <https://doi.org/10.1016/j.arabjc.2016.11.009>
- Su L., Zhang H., Oh K., Liu N., Luo Y., Cheng H., Zhang G. and He X. (2021). Activated biochar derived from spent *Auricularia auricula* substrate for the efficient adsorption of cationic azo dyes from single and binary adsorptive systems, *Water Science & Technology*, **84(1)**, 101–121, <https://doi.org/10.2166/wst.2021.222>
- Syafiuddin A., Salmiati S., Jonbi J. and Fulazzaky M.A. (2018). Application of the kinetic and isotherm models for better understanding of the behaviors of silver nanoparticles adsorption onto different adsorbents, *Journal of Environmental Management*, **15**, 59–70. <https://doi.org/10.1016/j.jenvman.2018.03.066>
- Tejada-Tovar C., Villabona-Ortiz A. and Gonzalez-Delgado A.D. (2021). Adsorption of Azo-Anionic Dyes in a Solution Using Modified Coconut (*Cocos nucifera*) Mesocarp: Kinetic and

- Equilibrium Study, *Water*, **13**, 1382, <https://doi.org/10.3390/w13101382>
- Velumsamy S., Roy A., Sundaram S. and Mallick T.K. (2021). A Review on Heavy Metal Ions and Containing Dyes Removal Through Graphene Oxide-Based Adsorption Strategies for Textile Wastewater Treatment, *The chemical record*, **21**, 1–42, <https://doi.org/10.1002/tcr.202000153>
- Venkatraman Y. and Priya A.K. (2021). Removal of heavy metal ion concentrations from the wastewater using tobacco leaves coated with iron oxide nanoparticles, *International Journal of Environmental Science and Technology*, **19**, 2721–2736, <https://doi.org/10.1007/s13762-021-03202-8>
- Vera L.M., Bermejo D., Uguna M.F., Flores M., Garcia N. and Gonzalez E. (2018). Fixed bed column modelling of lead (II) and cadmium (II) ions biosorption on sugarcane bagasse, *Environmental engineering research*, Doi: <https://doi.org/10.4491/eer.2018.042>
- Wang C., Wang X., Li N., Tao J., Yan B., Cui X. and Chen G. (2022). Adsorption of Lead from Aqueous Solution by Biochar: A Review, *Clean Technologies*, **4**, 629–652, <https://doi.org/10.3390/cleantechnol4030039>
- Wang Q., Liang L., Xi F., Tian G., Mao Q. and Meng X. (2020). Adsorption of Azo Dye Acid Red 73 onto Rice Wine Lees: Adsorption Kinetics and Isotherms, *Advances in Materials Science and Engineering*, ID–3469579. <https://doi.org/10.1155/2020/3469579>